PHOENICSユーザーカンファレンス2013
2013年10月11日(金)
東京国際フォーラム　ガラス棟6F G602

捻りテープ挿入円管内スワール流れによる乱流熱伝達の数値解析
―伝導底層厚さに及ぼすスワール流速の影響―

畑 幸一[1]、白井康之[2]、増崎　貴[3]、羽邑光道[4]
[1]京都大学エネルギー理工学研究所、[2]京都大学、[3]核融合科学研究所、[4]CHAM-Japan

1. 緒言

捻りテープ挿入円管(スワール管)内スワール流れによる伝導底層厚さの知識は、沸騰開始過熱度、核沸騰熱伝達、限界熱流束(DNB)過熱度を明らかにするために必要で、更に限界熱流束(CHF)発生機構を議論するために重要である。国際熱核融合実験炉(ITER)が採用するダイバータ部の高密度除熱方式は、水冷却平滑管内に金属製の捻りテープを挿入したスワール冷却管によるものである。

本研究では、汎用の熱流体解析コードPHOENICSを使用し、実験条件と同様に、捻りテープ挿入円管内スワール流れによる乱流熱伝達と圧力損失の数値解析を行い、実験的に導出した円管内水のスワール流れによる乱流熱伝達表示式、管摩擦係数表示式を検証し、スワール流速を種々変えたサブクール水の流動様式、伝導底層厚さ(δ_{CSL})を評価し、無次元伝導底層厚さ$(y^+_{CSL})_{TEM}$を明らかにした結果(1)を報告する。

円管内水の強制対流下の伝熱研究です。

プール沸騰熱伝達実験

その1. 水力的不安定性モデルに基づく限界熱流束

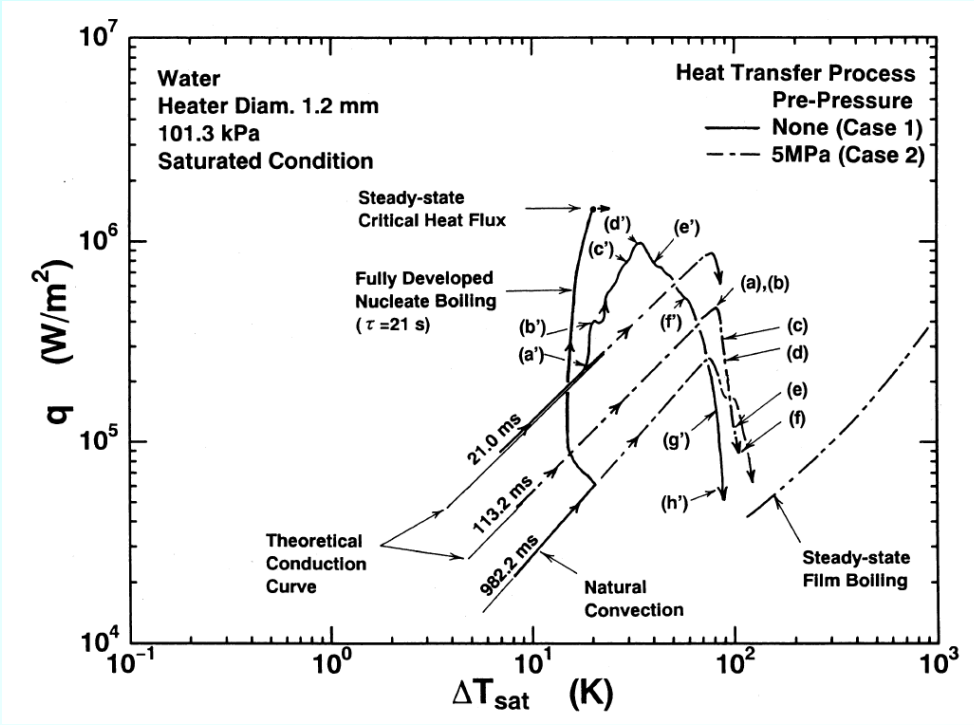

その2. 不均質自発核生成モデルに基づく限界熱流束

Experimental Data
- **Platinum**
- ***d*=1.2 mm**
- **L_{eff}=72 mm**
- ***P*=101.3 kPa**
- **Saturated Condition**
- **Pre-Pressure**
  - **None (Case 1)**
  - **5 MPa (Case 2)**

2. EXPERIMENTAL APPARATUS AND METHOD
2.1 Experimental water loop

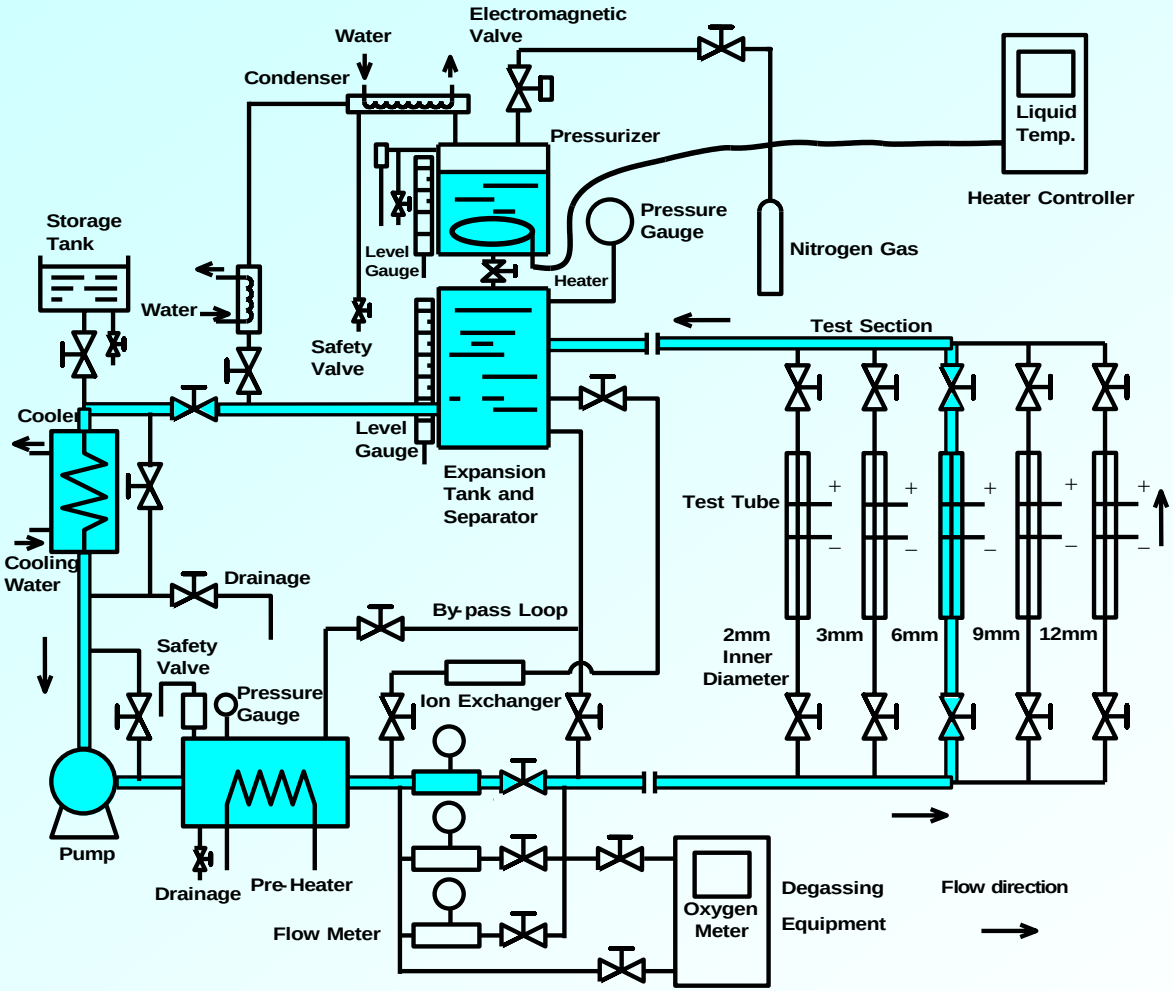

Fig. A Schematic diagram of experimental water loop.

2.2 Test section

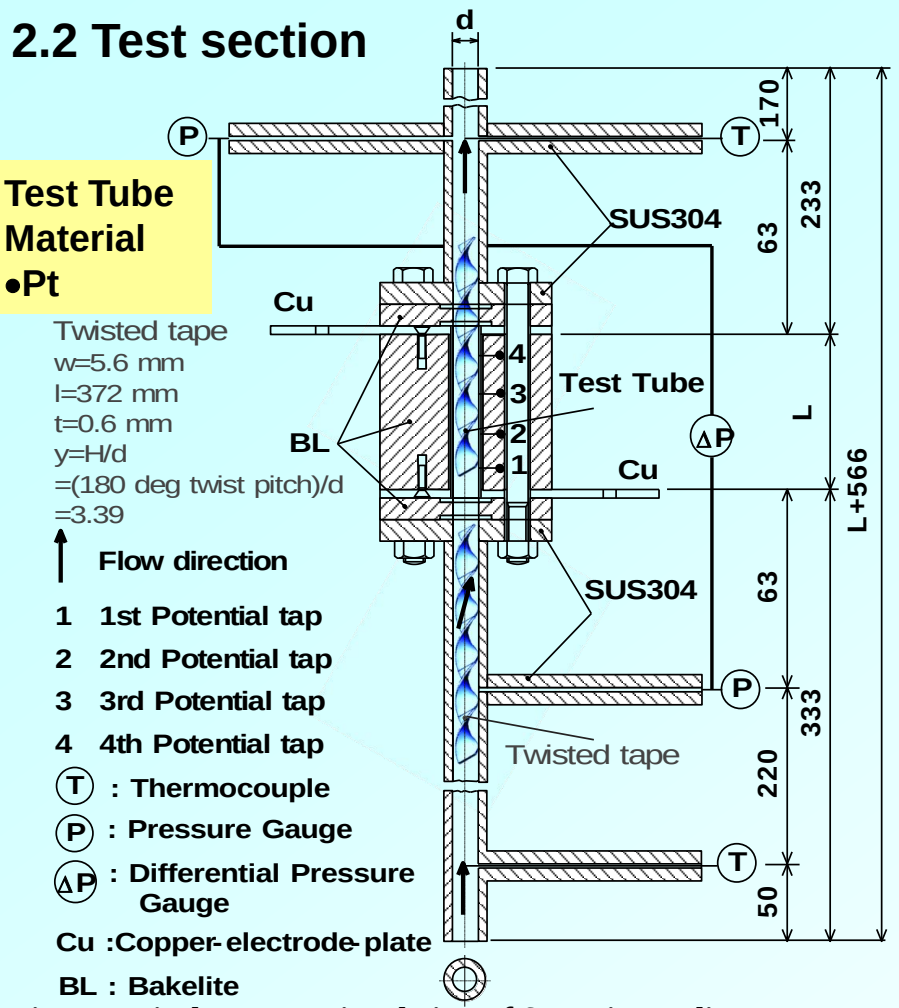

Test Tube Material
•Pt

Fig. BVertical cross-sectional view of 6 mm inner diameter test section with the twisted-tape insert.

The inlet and outlet pressures were calculated from the pressures measured by inlet and outlet pressure transducers as follows:

$$P_{in} = P_{ipt} - \left\{ \left(P_{ipt}\right)_{wnh} - \left(P_{opt}\right)_{wnh} \right\} \times \frac{L_{ipt}}{L_{ipt} + L + L_{opt}} \quad \text{(a)}$$

$$P_{out} = P_{in} - \left(P_{in} - P_{opt}\right) \times \frac{L}{L + L_{opt}} \quad \text{(b)}$$

where L_{ipt}=0.063 m and L_{opt}=0.063 m.

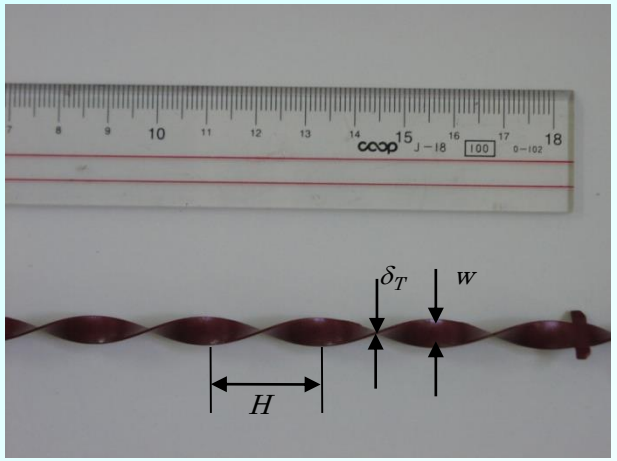

Fig. C Photograph of the SUS304 twisted-tape coated with alumina thermal spraying.

The swirl velocity, u_{sw}, was defined by the inlet flow velocity, u, in consideration of the decrement of flow cross section and the increment of flow length by the twisted-tape as follows [7-9]:

$$u_{sw} = u \frac{\pi d^2}{\pi d^2 - 4w\delta_T} \times \frac{(4y^2 + 2\pi^2)^{0.5}}{2y} \quad \text{(c)}$$

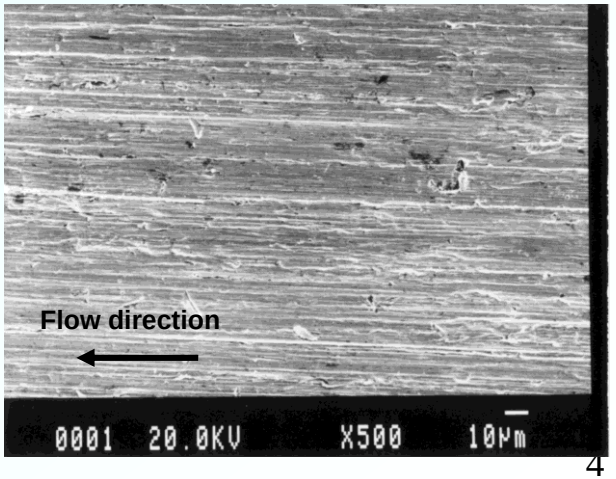

Fig. D SEM photograph of the Platinum test tube for an inner diameter of 6 mm with commercial finish of inner surface.

2.3 Method of heating test tube

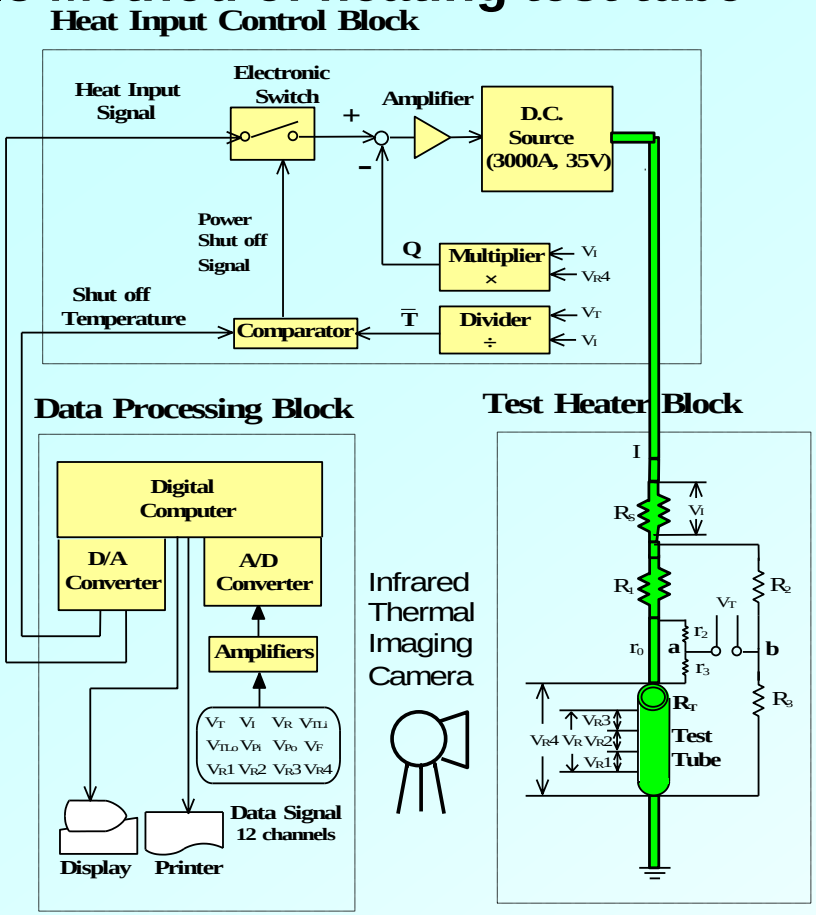

Fig. E Measurement and data processing system.

•The average temperature of the Pt test tube with twisted-tape insert was measured with resistance thermometry participating as a branch of a double bridge circuit for the temperature measurement.

•The average temperatures of the Pt test tube with twisted-tape insert between the first and forth potential taps and between adjacent potential taps (first and second potential taps, second and third ones, and third and forth ones) were calculated with the aid of previously calibrated resistance-temperature relation, respectively.

• The heat generation rates of the Pt test tube with twisted-tape insert between the first and forth potential taps and between adjacent potential taps were calculated from the measured voltage difference between the first and forth potential taps and between adjacent potential taps of the Pt test tube, and that across the standard resistance.

•The surface heat fluxes of the Pt test tube with twisted-tape insert between the first and forth potential taps and between adjacent potential taps are the differences between the heat generation rate per unit surface area and the rate of change of energy storage in the Pt test tube obtained from the faired average temperature versus time curve as follows:

$$q(t)=\frac{V}{S}\left(Q(t)-\rho c\frac{d\bar{T}}{dt}\right) \qquad \text{(d)}$$

•The heater inner surface temperatures of the Pt test tube with twisted-tape insert between the first and forth potential taps and between adjacent potential taps were also obtained by solving the steady one-dimensional heat conduction equation in the test tube under the conditions of measured average temperature and surface heat flux of the test tube. The solutions for the inner and outer surface temperatures of the Pt test tube with twisted-tape insert, T_s and T_{so}, are given as follows:

$$T_s=T(r_i)=\bar{T}-\frac{qr_i}{4(r_o^2-r_i^2)^2\lambda}\times\left[4r_o^2\left\{r_o^2\left(\ln r_o-\frac{1}{2}\right)-r_i^2\left(\ln r_i-\frac{1}{2}\right)\right\}-\left(r_o^4-r_i^4\right)\right]-\frac{qr_i}{2(r_o^2-r_i^2)\lambda}\left(r_i^2-2r_o^2\ln r_i\right) \qquad \text{(e)}$$

$$T_{so}=T(r_o)=\bar{T}-\frac{qr_i}{4(r_o^2-r_i^2)^2\lambda}\times\left[4r_o^2\left\{r_o^2\left(\ln r_o-\frac{1}{2}\right)-r_i^2\left(\ln r_i-\frac{1}{2}\right)\right\}-\left(r_o^4-r_i^4\right)\right]-\frac{qr_ir_o^2}{2(r_o^2-r_i^2)\lambda}\left(1-2\ln r_o\right) \qquad \text{(f)}$$

3. NUMERICAL SOLUTION OF TURBULENT HEAT TRANSFER

3.1 Fundamental Equations for k-ε Turbulence Model with High Reynolds Number Form

Theoretical equations for k-ε turbulence model [10] in a circular tube of d=6 mm with the twisted-tape insert shown in Fig. 3 were numerically solved by using PHOENICS code under the same conditions as the experimental ones.

(Transport Equation for k), Cylindrical coordinates (r, θ, z):

$$\rho\frac{\partial k}{\partial t}+\rho\frac{\partial}{\partial r}(v_r k)+\rho\frac{1}{r}\frac{\partial}{\partial \theta}(v_\theta k)+\rho\frac{\partial}{\partial z}(v_z k)=$$
$$\frac{1}{r}\frac{\partial}{\partial r}\left\{\left(\mu+\frac{\mu_t}{\sigma_k}\right)r\frac{\partial k}{\partial r}\right\}+\frac{1}{r^2}\frac{\partial}{\partial \theta}\left\{\left(\mu+\frac{\mu_t}{\sigma_k}\right)\frac{\partial k}{\partial \theta}\right\}+\frac{\partial}{\partial z}\left\{\left(\mu+\frac{\mu_t}{\sigma_k}\right)\frac{\partial k}{\partial z}\right\}+\rho(P_k+\Gamma_b-\varepsilon) \quad (1)$$

(Transport Equation for ε), Cylindrical coordinates (r, θ, z):

$$\rho\frac{\partial \varepsilon}{\partial t}+\rho\frac{\partial}{\partial r}(v_r \varepsilon)+\rho\frac{1}{r}\frac{\partial}{\partial \theta}(v_\theta \varepsilon)+\rho\frac{\partial}{\partial z}(v_z \varepsilon)=$$
$$\frac{1}{r}\frac{\partial}{\partial r}\left\{\left(\mu+\frac{\mu_t}{\sigma_\varepsilon}\right)r\frac{\partial \varepsilon}{\partial r}\right\}+\frac{1}{r^2}\frac{\partial}{\partial \theta}\left\{\left(\mu+\frac{\mu_t}{\sigma_\varepsilon}\right)\frac{\partial \varepsilon}{\partial \theta}\right\}+\frac{\partial}{\partial z}\left\{\left(\mu+\frac{\mu_t}{\sigma_\varepsilon}\right)\frac{\partial \varepsilon}{\partial z}\right\}+\rho\frac{\varepsilon}{k}(C_{1e}P_k+C_{3e}\Gamma_b-C_{2e}\varepsilon) \quad (2)$$

(Energy Equation), Cylindrical coordinates (r, θ, z):

$$\rho\frac{\partial h}{\partial t}+\rho\frac{\partial}{\partial r}(v_r h)+\rho\frac{1}{r}\frac{\partial}{\partial \theta}(v_\theta h)+\rho\frac{\partial}{\partial z}(v_z h)=$$
$$\frac{1}{r}\frac{\partial}{\partial r}\left\{\left(\lambda+c_p\frac{\mu_t}{\sigma_t}\right)r\frac{\partial T}{\partial r}\right\}+\frac{1}{r^2}\frac{\partial}{\partial \theta}\left\{\left(\lambda+c_p\frac{\mu_t}{\sigma_t}\right)\frac{\partial T}{\partial \theta}\right\}+\frac{\partial}{\partial z}\left\{\left(\lambda+c_p\frac{\mu_t}{\sigma_t}\right)\frac{\partial T}{\partial z}\right\}+Q \quad (3)$$

where $\nu_t = C_\mu k^{1/2} l_m$ (4), $\varepsilon = C_d \frac{k^{3/2}}{l_m}$ (5)

$$P_k=\nu_t\left[2\left\{\left(\frac{\partial v_r}{\partial r}\right)^2+\left(\frac{1}{r}\frac{\partial v_\theta}{\partial \theta}+\frac{v_r}{r}\right)^2+\left(\frac{\partial v_z}{\partial z}\right)^2\right\}+\left(\frac{1}{r}\frac{\partial v_r}{\partial \theta}+\frac{\partial v_\theta}{\partial r}-\frac{v_\theta}{r}\right)^2+\left(\frac{\partial v_\theta}{\partial z}+\frac{1}{r}\frac{\partial v_z}{\partial \theta}\right)^2+\left(\frac{\partial v_z}{\partial r}+\frac{\partial v_r}{\partial z}\right)^2\right] \quad (6)$$

$$\Gamma_b=\frac{-\nu_t}{\rho\sigma_t}\left(g_r\frac{\partial \rho}{\partial r}+g_\theta\frac{1}{r}\frac{\partial \rho}{\partial \theta}+g_z\frac{\partial \rho}{\partial z}\right) \quad (7), \qquad h = c_p T \quad (8)$$

$$\lambda_e=\lambda_t+\lambda \quad (9), \qquad \lambda_t=\frac{c_p\mu_t}{\sigma_t} \quad (10)$$

v_r, v_θ and v_z are the r, θ and z components of a velocity vector, respectively.

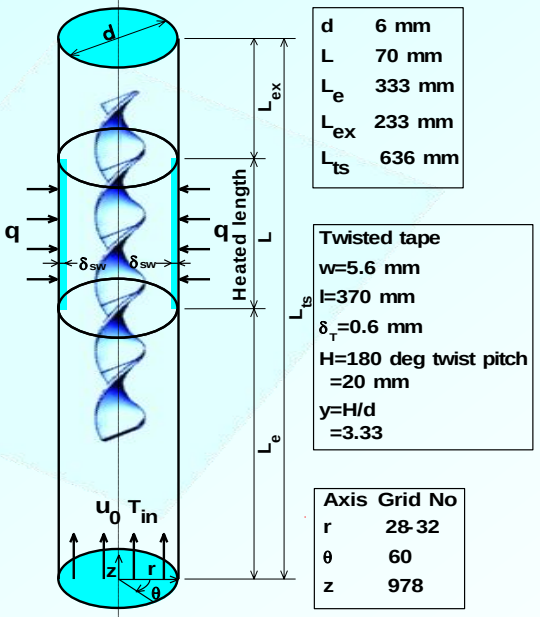

Fig. 2 Physical model for numerical analysis

3.2 Boundary conditions

The fundamental equations are numerically analyzed together with the following boundary conditions. On the outer boundary of heated section: constant heat flux, and non-slip condition.

$$q=-\lambda\frac{\partial T}{\partial r}=constant \quad (g)$$

At the outer boundary of non-heated section:

$$\frac{\partial T}{\partial r}=0 \quad (h)$$

At the lower boundary:

$T = T_{in}$, $v_r = 0$, $v_\theta = 0$ and $v_z = u$ for in-flow (i)

where T_{in} and u are a inlet liquid temperature and a flow velocity at the entrance of the test section.

3.3. Control volume cut-cell algorithm

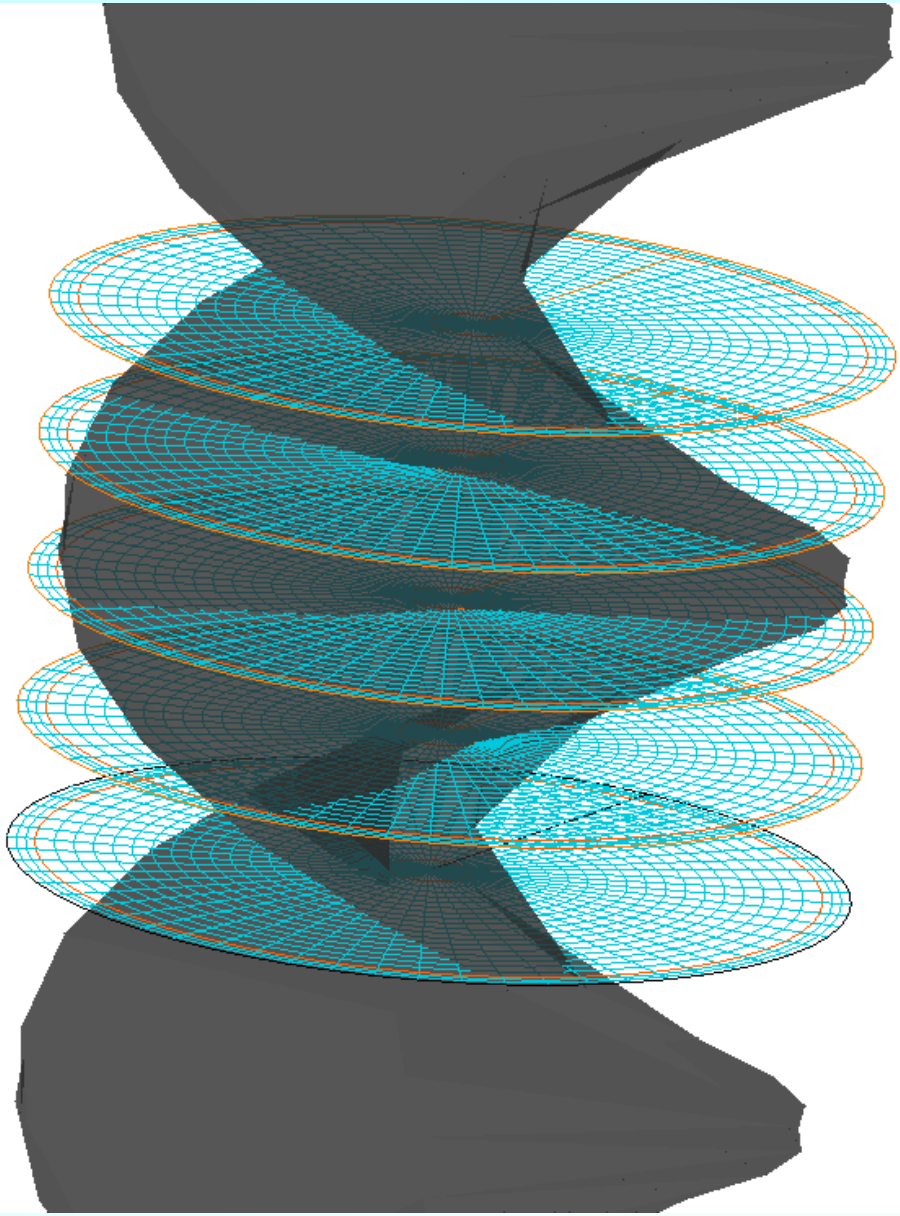

(I)

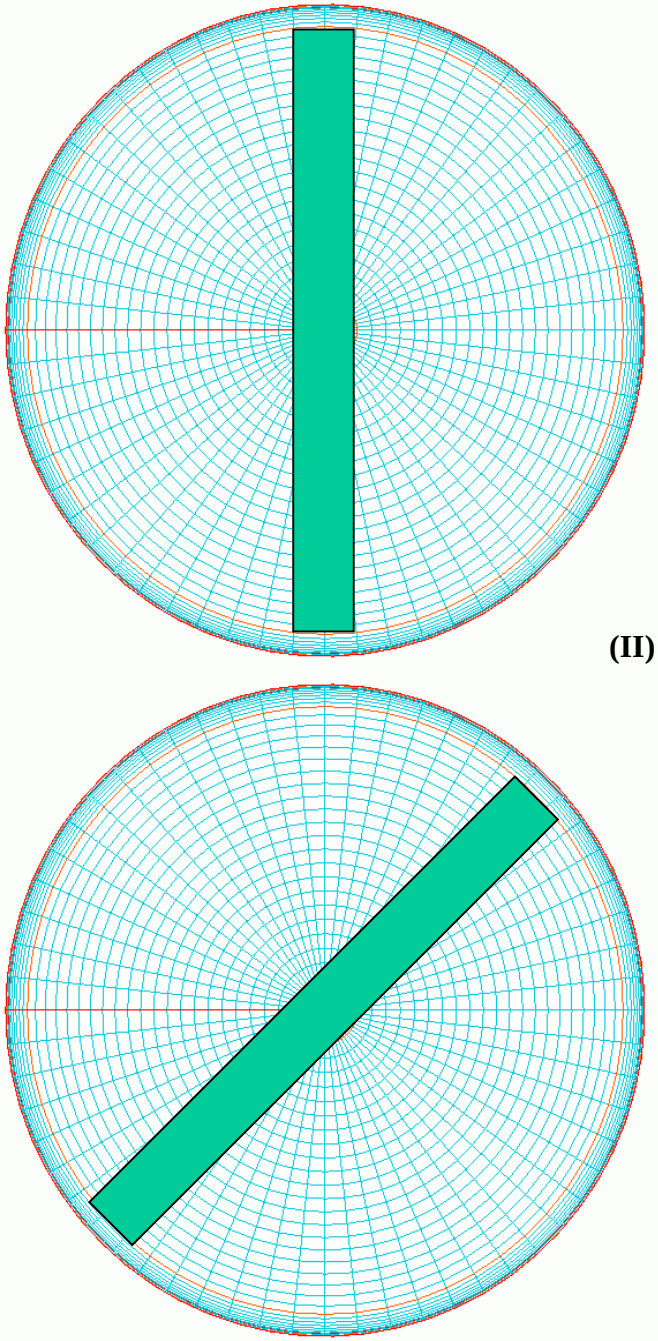

(II)

Fig. F twisted-tape 3D geometry-data for (I) into the PHOENICS-VR editor and (II) the cylindrical coordinate grid.

4. EXPERIMENTAL RESULTS AND DISCUSSION

4.1 Experimental Conditions and Parameters used for Calculation

Steady-state heat transfer processes that caused by exponentially increasing heat input, $Q_0 \exp(t/\tau)$, were measured for the Pt circular test tube with a SUS304 twisted-tape insert. The exponential periods, τ, of the heat input ranged from 6.04 to 22.33 s. The decrease of the exponential period means an increase in the rate of increasing heat input. The initial experimental conditions such as mass velocity, inlet liquid temperature, outlet pressure and exponential period for the pressure drop experiment and the turbulent heat transfer one were determined independently each other before each experimental run.

The experimental conditions were as follows:

Test Tube Number	THD-F169
Test Tube Material	Platinum
Inner Diameter (d)	6 mm
Heated Length (L)	69.6 mm
Wall thickness (δ)	0.4 mm
Effective Length (L_{eff})	59.2 mm
L/d	11.6
L_{eff}/d	9.87
L_{12} 19.6 mm, L_{23}	20.0 mm, L_{34} 19.6 mm
Surface condition	Commercial finish of inner surface
Surface roughness	0.45 for *Ra*, 2.93 for *Rmax* and 1.93 μm for *Rz*
Pump Input Frequency (f_{pi})	9.50 to 28.65 Hz
Mass Velocity (G)	4120 to 13570 kg/m^{2}s
Flow Velocity (u)	4.0, 6.9, 9.9 and 13.3 m/s
Axial Velocity (u_a)	4.51 to 15.08 m/s
Swirl Velocity (u_{sw})	5.39, 6.93, 13.38 and 18.03 m/s
Reynolds Number (Re_d)	2.379×10^4 to 8.582×10^4
Reynolds Number based on Swirl Velocity (Re_{sw})	3.913×10^4 to 1.572×10^5
Inlet Pressure (P_{in})	866.52 to 945.86 kPa
Outlet Pressure (P_{out})	852.27 to 858.04 kPa
Inlet Subcooling ($\Delta T_{sub,in}$)	144.68 to 147.05 K
Outlet Subcooling ($\Delta T_{sub,out}$)	132.05 to 139.81 K
Differential Pressure (ΔP)	9.416 to 76.681 kPa
Inlet Liquid Temperature (T_{in})	300.13 to 305.78 K
Exponentially Increasing Heat Input (Q)	$Q_0 \exp(t/\tau)$, τ=6.04 to 22.33 s

Twisted-Tape Number	TT2
Twisted-Tape Material	SUS304
Width (w)	5.6 mm
Thickness (δ_T)	0.6 mm,
Total Length (l)	372 mm
Pitch of 180° rotation (H)	20.34 mm
Twist Ratio [$y=H/d$=(pitch of 180° rotation)/d]	3.39
Electric Insulation	Alumina thermal spraying

4. EXPERIMENTAL RESULTS AND DISCUSSION

4.1 Experimental Conditions and Parameters used for Calculation

The parameters used for calculation were as follows:

Inner diameter (d)	6 mm
Heated length (L)	70 mm
Entrance length (L_e)	333 mm
Exit length (L_{ex})	233 mm
Test section length (L_{ts})	636 mm
Heat flux (q)	2.69×10^5 to 2.77×10^7 W/m^2 ($q_0\, exp(t/\tau)$, τ=20.04 to 21.14 s)
Inlet flow velocity (u)	4.134, 7.225, 10.05 and 13.628 m/s
Inlet liquid temperature (T_{in})	300.13 to 305.78 K
Coordinate system	cylindrical coordinate (r, θ, z)
Control volume	number (28 to 32, 60, 978) cut-cell algorithm
Physical model	k-ε turbulence model with high Reynolds number form
Twisted-Tape	solid with smooth-wall friction
Width (w)	5.6 mm
Thickness (δ_T)	0.6 mm,
Total Length (l)	370 mm
Pitch of 180° rotation (H)	20 mm
Twist Ratio	3.33

4.2. Inlet and Outlet Pressures, P_{in} and P_{out}, and Pressures Measured by the Inlet and Outlet Pressure Transducers, P_{ipt} and P_{opt} for TTI Tube

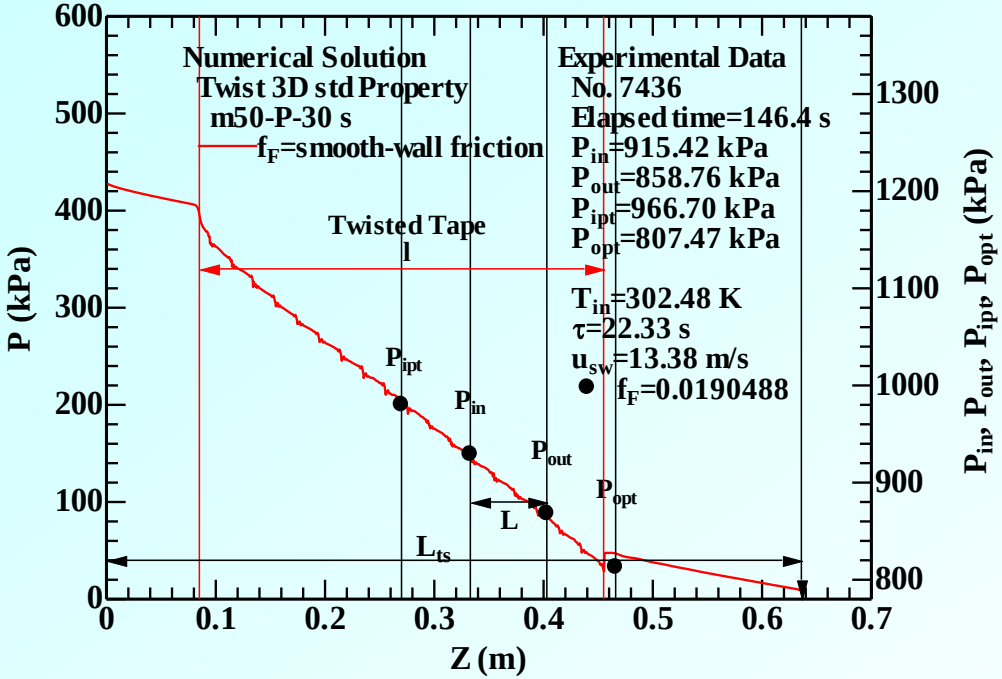

Fig. 3 *Z*-axis distributions of pressures measured, P_{ipt}, P_{opt}, P_{in} and P_{out}, for T_{in}=302.48 K, u_{sw}=13.38 m/s and f_F=0.019 compared with numerical solutions of liquid pressure, *P*.

The inlet and outlet pressures for the test tube with the twisted-tape insert were calculated from the pressures measured by inlet and outlet pressure transducers as follows:

$$P_{in} = P_{ipt} - \left\{ \left(P_{ipt}\right)_{wnh} - \left(P_{opt}\right)_{wnh} \right\} \times \frac{L_{ipt}}{L_{ipt} + L + L_{opt}} \qquad \text{(a)}$$

$$P_{out} = P_{in} - \left(P_{in} - P_{opt}\right) \times \frac{L}{L + L_{opt}} \qquad \text{(b)}$$

where L_{ipt}=0.063 m and L_{opt}=0.063 m.

4.3. Inner and Outer Surface Temperatures, T_s and T_{so}, Heat Fluxes, q, and Heat Transfer Coefficients, h, for 1st, 2nd and 3rd Positions of Three Sections, and Inlet and Outlet Liquid Temperatures, T_{in} and T_{out}, for TTI Tube

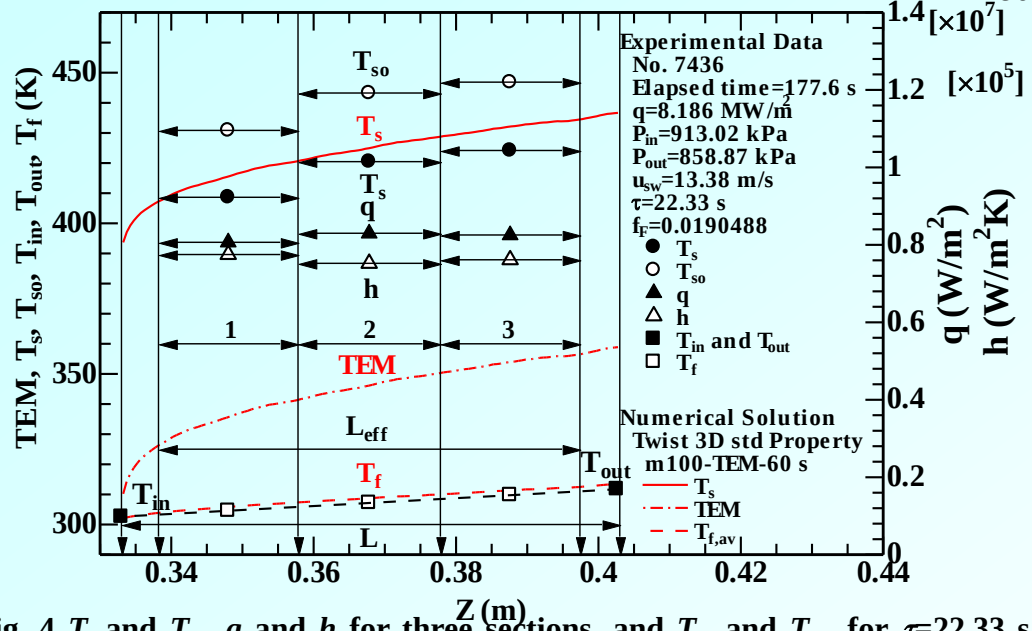

Fig. 4 T_s and T_{so}, q and h for three sections, and T_{in} and T_{out} for τ=22.33 s at u_{sw}=13.38 m/s compared with numerical solutions of *TEM*, T_{in} and T_{out}.

The temperatures of the heater inner and outer surfaces, T_s and T_{so}, on the test tube with twisted-tape insert can be described as follows:

$$T_s = T(r_i) = \bar{T} - \frac{qr_i}{4(r_o^2 - r_i^2)^2 \lambda} \times \left[4r_o^2 \left\{ r_o^2 \left(\ln r_o - \frac{1}{2} \right) - r_i^2 \left(\ln r_i - \frac{1}{2} \right) \right\} - \left(r_o^4 - r_i^4 \right) \right] - \frac{qr_i}{2(r_o^2 - r_i^2)\lambda} \left(r_i^2 - 2r_o^2 \ln r_i \right) \quad \text{(e)}$$

$$T_{so} = T(r_o) = \bar{T} - \frac{qr_i}{4(r_o^2 - r_i^2)^2 \lambda} \times \left[4r_o^2 \left\{ r_o^2 \left(\ln r_o - \frac{1}{2} \right) - r_i^2 \left(\ln r_i - \frac{1}{2} \right) \right\} - \left(r_o^4 - r_i^4 \right) \right] - \frac{qr_i r_o^2}{2(r_o^2 - r_i^2)\lambda} \left(1 - 2 \ln r_o \right) \quad \text{(f)}$$

The surface temperatures on the test tube with twisted-tape insert, T_s, were calculated from the analyzed liquid temperature of the outer control volume on the test tube surface, *TEM*, which is supposed to be located on the center of the control volume, by solving the heat conduction equation in liquid as given in Eq. (j).

$$T_s = q(\Delta r)_{out} / 2\lambda_l + TEM \quad \text{(j)}$$

The average liquid temperatures, $T_{f,av}$, were calculated from the analyzed liquid temperatures of the control volumes on the r and θ-axis grid numbers for each z-axis grid number. Those become linearly higher with an increase in the z-axis distance, Z, and become almost equal to the outlet liquid temperature, T_{out}, at the exit of the heated length.

4.4. Steady-state Turbulent Heat Transfer Characteristics for TTI Tube

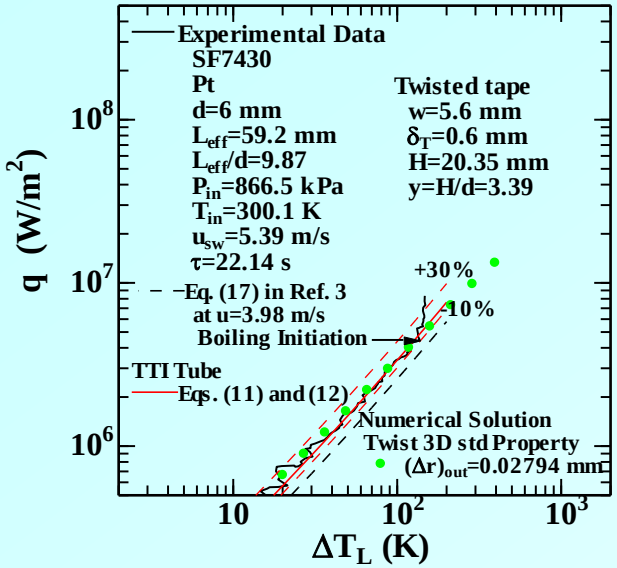

Fig. G Relationship between q and ΔT_L [=$(T_{s,av}$-$T_l)$] for circular tube of d=6 mm and L_{eff}=59.2 mm with twisted-tape of y=3.39 on u_{sw}=5.39 m/s at P_{in}=867 kPa.

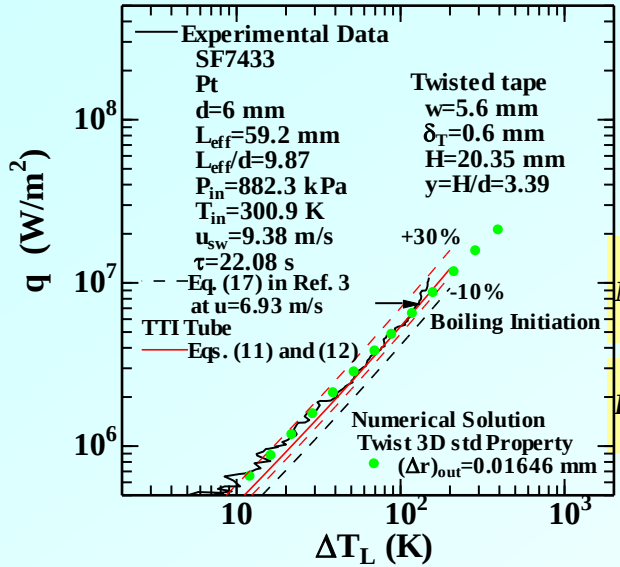

Fig. H Relationship between q and ΔT_L [=$(T_{s,av}$-$T_l)$] for circular tube of d=6 mm and L_{eff}=59.2 mm with twisted-tape of y=3.39 on u_{sw}=9.38 m/s at P_{in}=882 kPa.

Authors' steady-state turbulent heat transfer correlations for the circular tubes with various twisted-tape inserts

$$Nu_d = 0.02\,Re_{sw}^{0.85}\,Pr^{0.4}\left(\frac{L_{eff}}{d}\right)^{-0.08}\left(\frac{\mu_l}{\mu_w}\right)^{0.14} \quad (11)$$

$$Re_{sw} = Re_d\,\frac{\pi d^2}{\pi d^2 - 4w\delta_T} \times \frac{(4y^2 + 2\pi^2)^{0.5}}{2y} \quad (12)$$

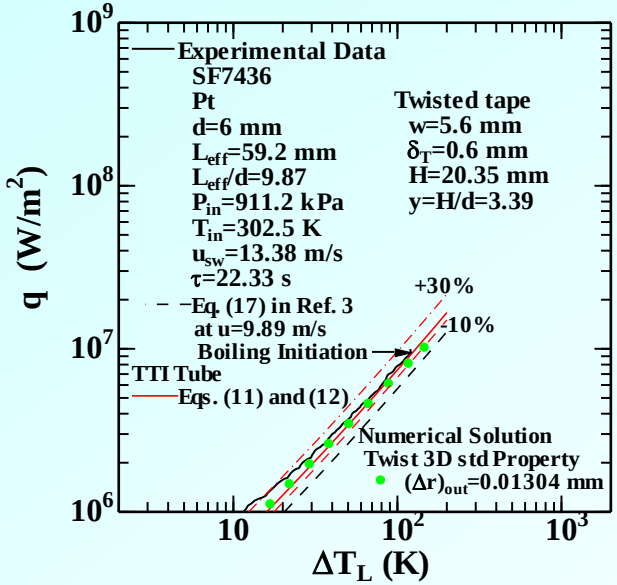

Fig. 5 Relationship between q and ΔT_L [=$(T_{s,av}$-$T_l)$] for circular tube of d=6 mm and L_{eff}=59.2 mm with twisted-tape of y=3.39 on u_{sw}=13.38 m/s at P_{in}=911 kPa.

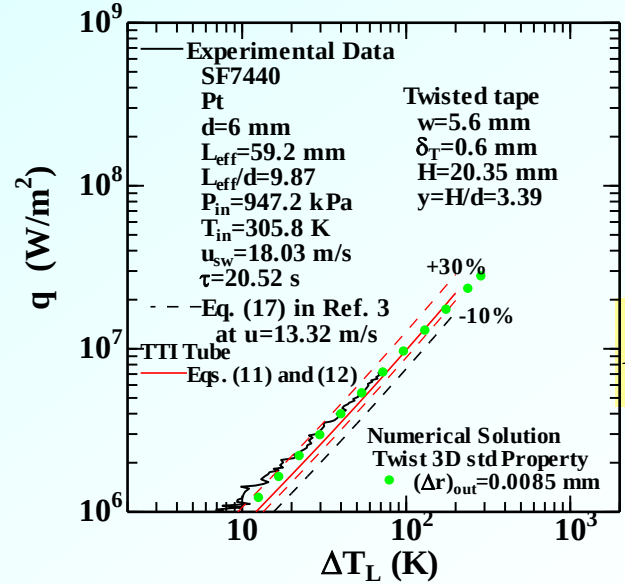

Fig. I Relationship between q and ΔT_L [=$(T_{s,av}$-$T_l)$] for circular tube of d=6 mm and L_{eff}=59.2 mm with twisted-tape of y=3.39 on u_{sw}=18.03 m/s at P_{in}=947 kPa.

Authors' steady-state turbulent heat transfer correlation for the empty circular tube

$$Nu_d = 0.02\,Re_d^{0.85}\,Pr^{0.4}\left(\frac{L}{d}\right)^{-0.08}\left(\frac{\mu_l}{\mu_w}\right)^{0.14}$$

(17) in Ref. 3

4.4. Steady-state Turbulent Heat Transfer Characteristics for TTI Tube

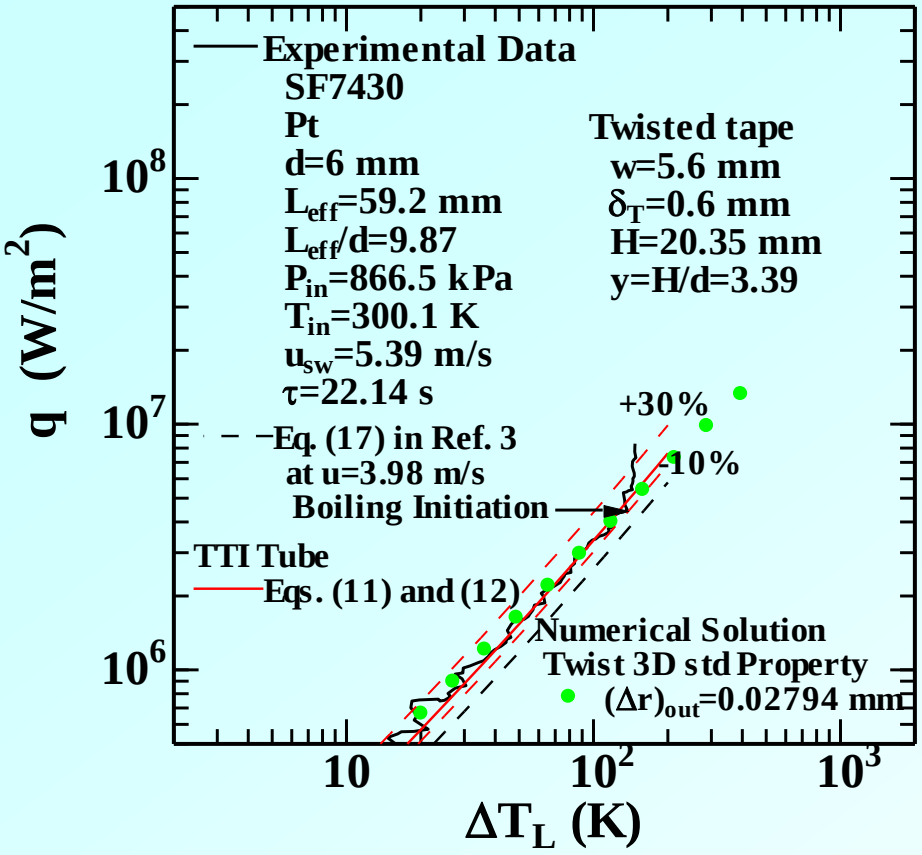

Fig. G Relationship between q and ΔT_L [=$(T_{s,av}$-$T_L)$] for circular tube of d=6 mm and L_{eff}=59.2 mm with twisted-tape of y=3.39 on u_{sw}=5.39 m/s at P_{in}=867 kPa.

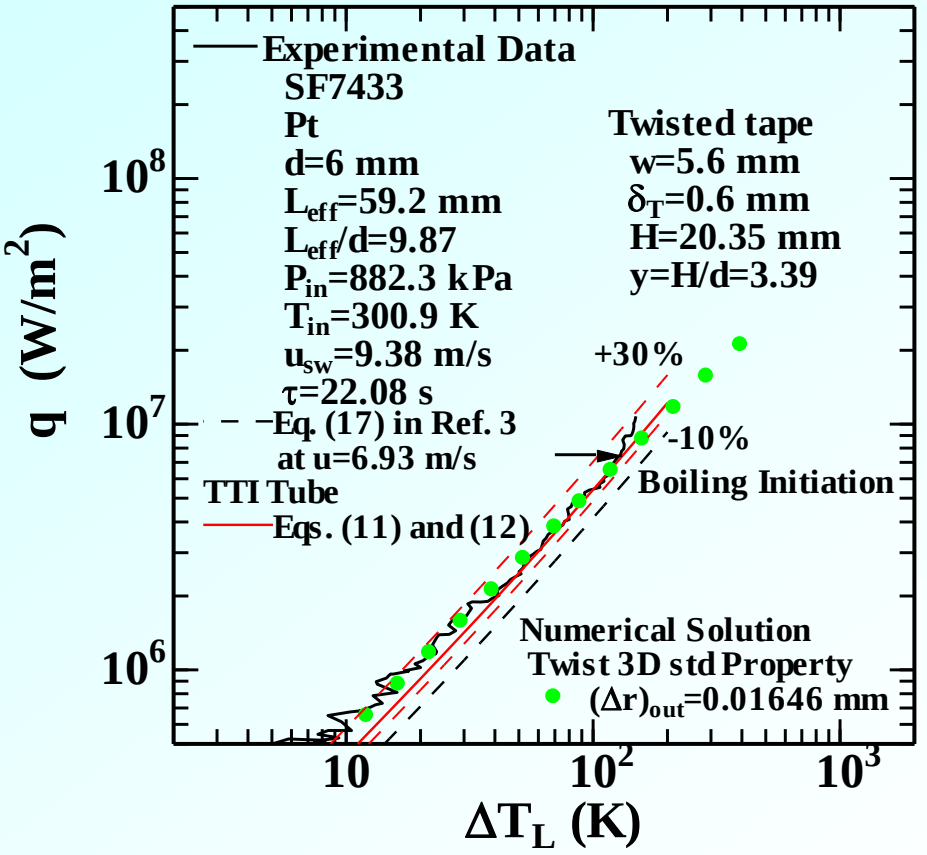

Fig. H Relationship between q and ΔT_L [=$(T_{s,av}$-$T_L)$] for circular tube of d=6 mm and L_{eff}=59.2 mm with twisted-tape of y=3.39 on u_{sw}=9.38 m/s at P_{in}=882 kPa.

Authors' steady-state turbulent heat transfer correlations for the circular tubes with various twisted-tape inserts

$$Nu_d = 0.02\, Re_{sw}^{0.85}\, Pr^{0.4} \left(\frac{L_{eff}}{d}\right)^{-0.08} \left(\frac{\mu_l}{\mu_w}\right)^{0.14} \quad (11)$$

$$Re_{sw} = Re_d \frac{\pi d^2}{\pi d^2 - 4w\delta_T} \times \frac{(4y^2 + 2\pi^2)^{0.5}}{2y} \quad (12)$$

Authors' steady-state turbulent heat transfer correlation for the empty circular tube

$$Nu_d = 0.02\, Re_d^{0.85}\, Pr^{0.4} \left(\frac{L}{d}\right)^{-0.08} \left(\frac{\mu_l}{\mu_w}\right)^{0.14} \quad (17) \text{ in Ref. 3}$$

4.4. Steady-state Turbulent Heat Transfer Characteristics for TTI Tube

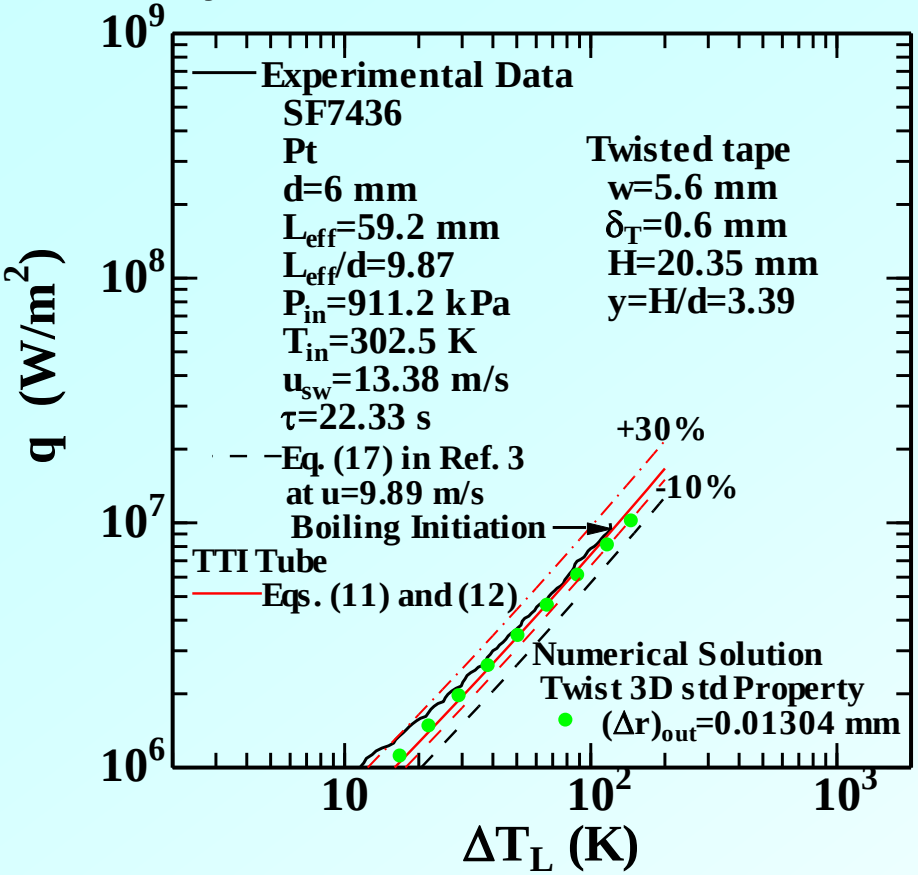

Fig. 5 Relationship between q and ΔT_L [$=(T_{s,av}-T_L)$] for circular tube of d=6 mm and L_{eff}=59.2 mm with twisted-tape of y=3.39 on u_{sw}=13.38 m/s at P_{in}=911 kPa.

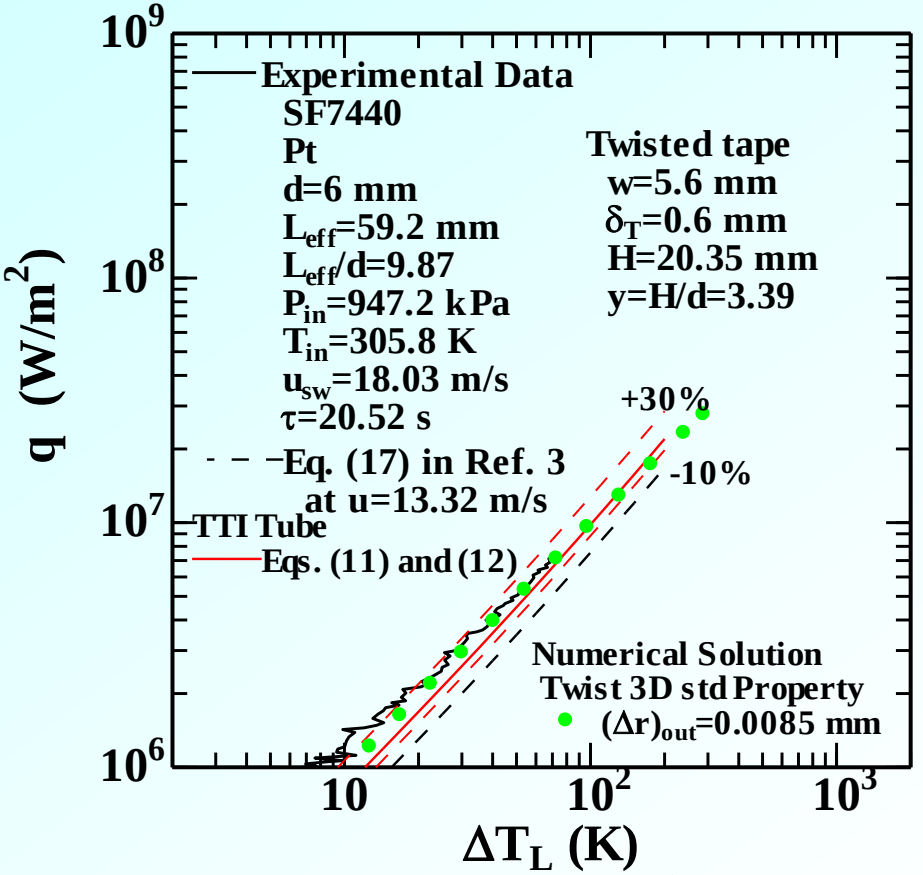

Fig. I Relationship between q and ΔT_L [$=(T_{s,av}-T_L)$] for circular tube of d=6 mm and L_{eff}=59.2 mm with twisted-tape of y=3.39 on u_{sw}=18.03 m/s at P_{in}=947 kPa.

Authors' steady-state turbulent heat transfer correlations for the circular tubes with various twisted-tape inserts

$$Nu_d = 0.02\,Re_{sw}^{0.85}\,Pr^{0.4}\left(\frac{L_{eff}}{d}\right)^{-0.08}\left(\frac{\mu_l}{\mu_w}\right)^{0.14} \quad (11)$$

$$Re_{sw} = Re_d\,\frac{\pi d^2}{\pi d^2 - 4w\delta_T}\times\frac{(4y^2+2\pi^2)^{0.5}}{2y} \quad (12)$$

Authors' steady-state turbulent heat transfer correlation for the empty circular tube

$$Nu_d = 0.02\,Re_d^{0.85}\,Pr^{0.4}\left(\frac{L}{d}\right)^{-0.08}\left(\frac{\mu_l}{\mu_w}\right)^{0.14}$$ (17) in Ref. 3

4.5. Thickness of Conductive Sub-layer, δ_{CSL}, and the Non-dimensional Thickness of Conductive Sub-layer, y^+_{CSL}, for Steady-state Turbulent Heat Transfer on TTI Tube

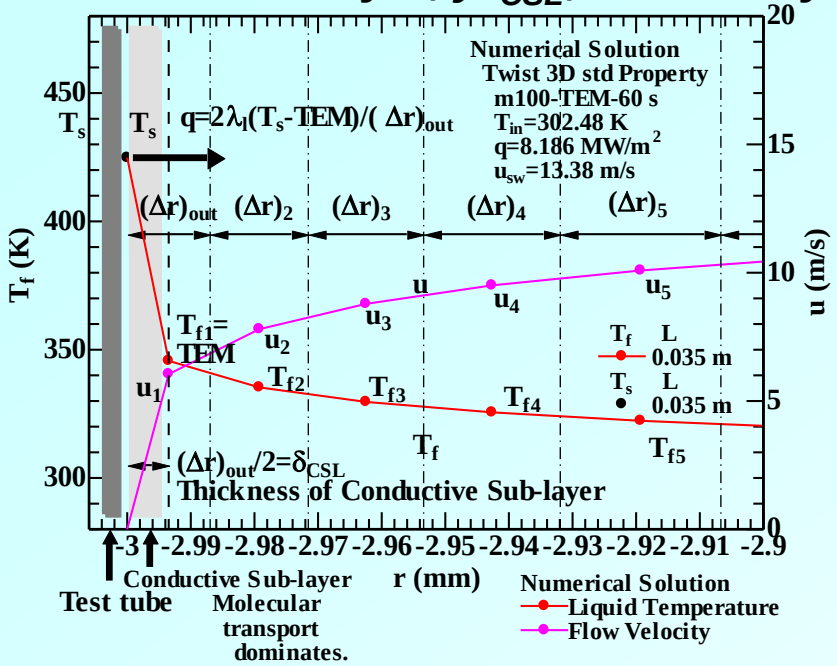

Fig. J Liquid temperatures in the conductive sub-layer for circular tube of *d*=6 mm with twisted-tape insert.

The liquid temperatures on the test tube surface in the conductive sub-layer will become linearly lower with a decrease in the radius by the heat conduction from the surface temperature on the test tube with twisted-tape insert, $T_f=T_s-\Delta rq/\lambda_l$. And let those, T_f, equal the analyzed temperature of the outer control volume on the test tube surface, ***TEM***, in the inner region of the turbulent flow, which is supposed to be located on the center of the control volume as given in $T_f=T_s-(\Delta r)_{out}q/2\lambda_l=TEM$. Half the thickness of the outer control volume, $(\Delta r)_{out}/2$, would become the thickness of the conductive sub-layer, δ_{CSL}, for the turbulent heat transfer in a vertical circular tube under two-phase model classified into conductive sub-layer and inner region of the turbulent flow.

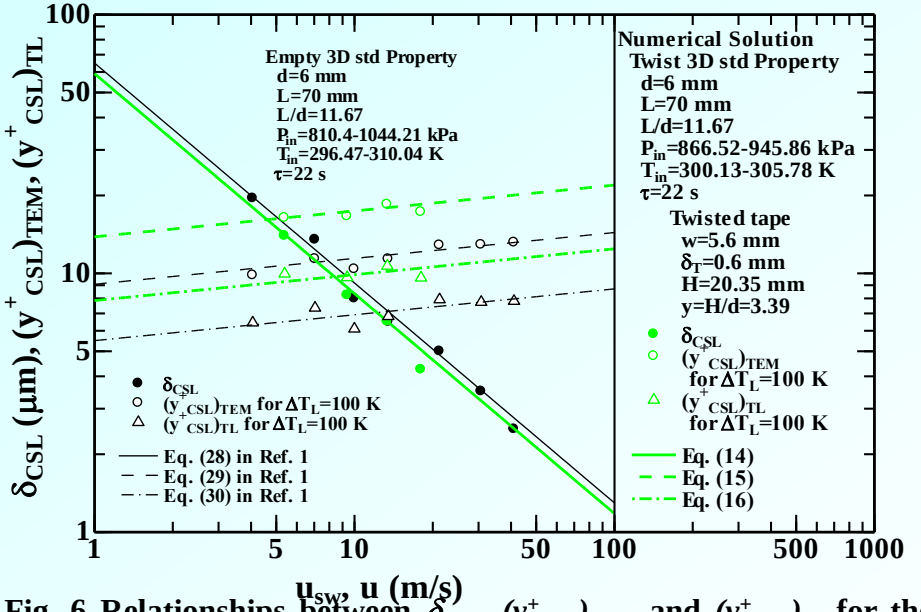

Fig. 6 Relationships between δ_{CSL}, $(y^+_{CSL})_{TEM}$ and $(y^+_{CSL})_{TL}$ for the turbulent heat transfer numerically solved, and u_{sw} with ΔT_L=100 K.

These numerical solutions of δ_{CSL}, $(y^+_{CSL})_{TEM}$ and $(y^+_{CSL})_{TL}$ for the circular tube with the twisted-tape of y=3.33 for the u_{sw} of 5.39, 9.38, 13.38 and 18.03 m/s can be expressed by the following correlations:

$$\delta_{CSL} = 59.12\times10^{-6}\,u_{sw}^{-0.85} \qquad (14)$$

$$(y^+_{CSL})_{TEM} = 13.84\,u_{sw}^{0.1} \quad \text{for } \Delta T_L=100 \text{ K} \qquad (15)$$

$$(y^+_{CSL})_{TL} = 7.85\,u_{sw}^{0.1} \quad \text{for } \Delta T_L=100 \text{ K} \qquad (16)$$

Equation (14), $1/\delta_{CSL}\propto u_{sw}^{0.85}$, represents authors' steady-state turbulent heat transfer correlation for the circular tubes with various twisted-tape inserts, Eq. (11), derived from the experimental data.

$$Nu_d = 0.02\,Re_{sw}^{0.85}\,Pr^{0.4}\left(\frac{L_{eff}}{d}\right)^{-0.08}\left(\frac{\mu_l}{\mu_w}\right)^{0.14} \qquad (11)$$

4.5. Thickness of Conductive Sub-layer, δ_{CSL}, and the Non-dimensional Thickness of Conductive Sub-layer, y^+_{CSL}, for Steady-state Turbulent Heat Transfer on TTI Tube

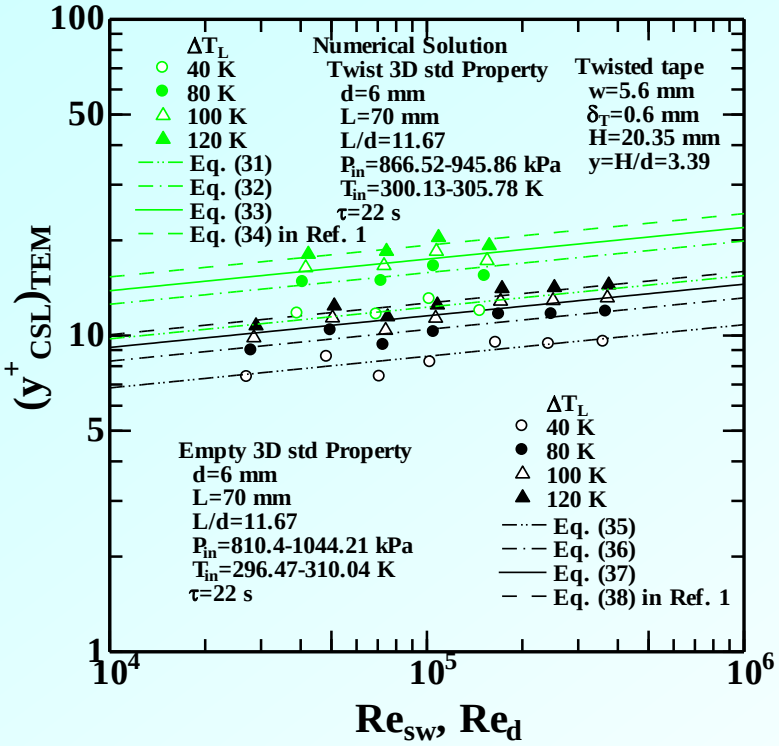

Fig. K Relationship between $(y^+_{CSL})_{TEM}$ for the turbulent heat transfer numerically solved, and Re_{sw} with ΔT_L=40, 80, 100 and 120 K.

These numerical solutions of $(y^+_{CSL})_{TEM}$ are also shown versus Reynolds number based on swirl velocity and Reynolds number, Re_{sw} and Re_d, with the temperature differences between average inner surface temperature and liquid bulk mean temperature, ΔT_L, of 40, 80, 100 and 120 K as green symbols in Fig. K. These numerical solutions of $(y^+_{CSL})_{TEM}$ for the circular tube with the twisted-tape of y=3.33 can be expressed for the Re_{sw} ranging from 3.913×10^4 to 1.572×10^5 by the following correlations:

$(y^+_{CSL})_{TEM} = 3.89\,Re_{sw}^{0.1}$ for ΔT_L=40 K (31) in Ref. 1, $(y^+_{CSL})_{TEM} = 5.00\,Re_{sw}^{0.1}$ for ΔT_L=80 K (32) in Ref. 1

$(y^+_{CSL})_{TEM} = 5.52\,Re_{sw}^{0.1}$ for ΔT_L=100 K (33) in Ref. 1, $(y^+_{CSL})_{TEM} = 6.10\,Re_{sw}^{0.1}$ for ΔT_L=120 K (34) in Ref. 1

5. 結言

3分割したPtスワール管発熱体を直接通電する方法で、広範囲のスワール流速、発熱体表面温度と液温との差において局所及び平均乱流熱伝達、発熱体入口及び出口液温、局所発熱体表面温度、圧力損失を実験計測し、実験と同様な条件で数値解析した。

スワール管内水の乱流熱伝達表示式(11)、(12) [4]は実験結果及び数値解析結果を0～+20 %以内の誤差で表示する。また、発熱体に接する伝導底層厚さδ_{CSL}は流速の増加とともに直線的に減少するが、無次元伝導底層厚さy^{+}_{CSL}はほぼ一定の値である。

参考文献 K. Hata, Y. Shirai, S. Masuzaki and A. Hamura, “Computational Study of Twisted-Tape-Induced Swirl Flow Heat Transfer and Pressure Drop in a Vertical Circular Tube under Velocities Controlled,” *Nuclear Engineering and Design*, **263**, pp. 443-455, 2013.

Nuclear Engineering and Design 263 (2013) 443–455

Contents lists available at SciVerse ScienceDirect

Nuclear Engineering and Design

journal homepage: www.elsevier.com/locate/nucengdes

Computational study of twisted-tape-induced swirl flow heat transfer and pressure drop in a vertical circular tube under velocities controlled

K. Hata[a,*], Y. Shirai[b], S. Masuzaki[c], A. Hamura[d]

[a] Institute of Advanced Energy, Kyoto Univ. Gokasho, Uji, Kyoto 611-0011, Japan
[b] Department of Energy Science and Technology, Kyoto Univ. Sakyo-ku, Kyoto 606-8501, Japan
[c] National Institute for Fusion Science, 322-6 Oroshi-cho, Toki, Gifu 509-5292, Japan
[d] Concentration Heat and Momentum Ltd. , 3-5-4 Koji-machi, Chiyoda-ku, Tokyo 102-0083, Japan

HIGHLIGHTS

- Measure turbulent heat transfer coefficients in a pipe with twisted-tape insert.
- Use a Pt pipe of 6 mm ID and a SUS304 twisted-tape with twist ratio of 3.39.
- Solve numerically turbulent heat transfer in a pipe with twisted-tape insert.
- Numerical solutions are in good agreement with experimental data.
- Clarify thickness of conductive sub-layer in a pipe with twisted-tape insert.

ARTICLE INFO

Article history:
Received 24 January 2013
Received in revised form 27 May 2013
Accepted 30 May 2013

ABSTRACT

The twisted-tape-induced swirl flow heat transfer due to exponentially increasing heat inputs with various exponential periods and twisted-tape-induced pressure drop were systematically measured with mass velocity $G = 4120$ to $13\,570\ kg/m^2/s$, inlet liquid temperature $T_{in} = 300.13$ to $305.78\ K$ and inlet pressure $P_{in} = 866.52$ to $945.86\ kPa$ by an experimental water loop flow. Measurements were made on a 59.2 mm effective length and its three sections (upper, mid and lower positions), which were spot-welded four potential taps on the outer surface of a 6 mm inner diameter, a 69.6 mm heated length and a 0.4 mm thickness of Platinum circular test tube with the twisted-tape insert. The SUS304 twisted-tape of width $w = 5.6$ mm, thickness $\delta_T = 0.6$ mm, total length $l = 372$ mm, pitch of 180° rotation $H = 20.34$ mm and twist ratio $y = H/d = 3.39$ was employed in this work. On the other hand, theoretical equations for $k-\varepsilon$ turbulence model in a circular tube of a 6 mm in diameter and a 636 mm long with the twisted-tape insert were numerically solved for heating of water with heated section of a 6 mm in diameter and a 70 mm long by using PHOENICS code under the same conditions as the experimental ones considering the temperature dependence of thermo-physical properties concerned. The twisted-tape of $w = 5.6$ mm, $\delta_T = 0.6$ mm, $l = 370$ mm, $H = 20$ mm and $y = 3.33$ was installed under the same experimental position. The surface heat flux q and the average surface temperature T_{sav} on the circular tube with the twisted-tape of $y = 3.33$ obtained theoretically were compared with the corresponding experimental values on q versus the temperature difference between average heater inner surface temperature and liquid bulk mean temperature ΔT_L [$=T_{sav} - T_L$, $T_L = (T_{in} + T_{out})/2$] graph. The numerical solutions of q and ΔT_L are almost in good agreement with the corresponding experimental values of q and ΔT_L with the deviations less than 0% to +20% for the range of ΔT_L tested here. The numerical solutions of the local surface temperature $\langle T_s \rangle_Z$, local average liquid temperature $\langle T_{fav} \rangle_Z$ and local liquid pressure drop ΔP_Z were also compared with the corresponding experimental data of $\langle T_s \rangle_Z$, $\langle T_{fav} \rangle_Z$ and ΔP_Z versus heated length L or distance from inlet of the test section Z graph, respectively. The numerical solutions of $\langle T_s \rangle_Z$, $\langle T_{fav} \rangle_Z$ and ΔP_Z are within ±5% difference of the corresponding experimental data on $\langle T_s \rangle_Z$, $\langle T_{fav} \rangle_Z$ and ΔP_Z. The thickness of

* Corresponding author. Tel.: +81 774 38 3473; fax: +81 774 38 3473.
E-mail addresses: hata@iae.kyoto-u.ac.jp (K. Hata), shirai@pe.energy.kyoto-u.ac.jp (Y. Shirai), Japanmasuzaki@LHD.nifs.ac.jp (S. Masuzaki), hamura@phoenics.co.jp (A. Hamura).

0029-5493/$ – see front matter
http://dx.doi.org/10.1016/j.nucengdes.2013.05.027

This is my way of approaching CHF in Circular Tube with Twisted-Tape Insert

1. Fixed Pump Power, PP_{pump}, and Fixed Pump Discharge Pressure, P_{pumpd}

Circular Tube

Mass Velocity $G=\rho u$ kg/m^{2}s
Flow Velocity u m/s
Conductive Sub-Layer δ μm
δ is induced by u.

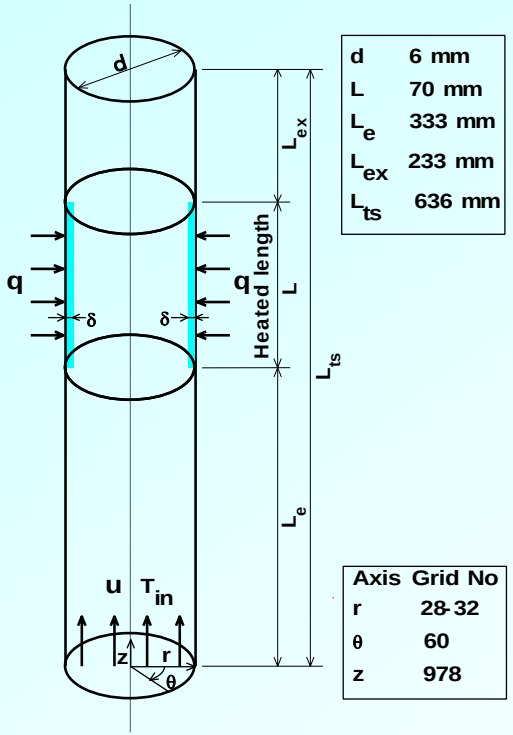

Fixed PP_{pump}, P_{pumpd} or Fixed G

Circular Tube with Twisted-Tape Insert

Mass Velocity $G_{sw}=\rho u_{ax,sw}$ kg/m^{2}s
Axial Flow Velocity $u_{ax,sw}$ m/s
Swirl Velocity u_{sw} m/s
Conductive Sub-Layer δ_{sw} μm
δ_{sw} is induced by u_{sw}.

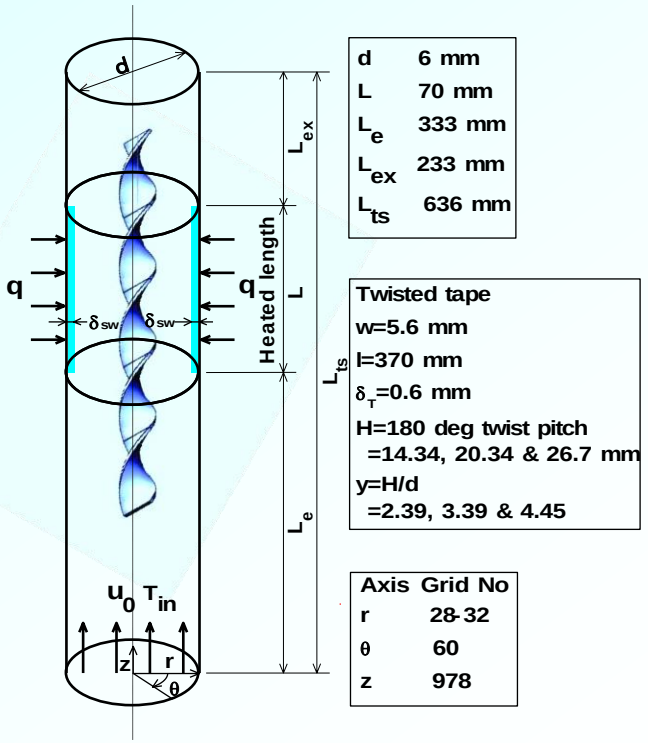

Fixed $PP_{pump,sw}$, $P_{pumpd,sw}$ or Fixed G_{sw}

This is my way of approaching CHF in Circular Tube with Twisted-Tape Insert

1. Fixed Pump Power, PP_{pump}, and Fixed Pump Discharge Pressure, P_{pumpd}

Twist-Tap is Flow Resistance.

$G>G_{sw}$

$u>u_{ax,sw}$

The swirl velocity, u_{sw}, was defined by the inlet flow velocity, u_0, in consideration of the decrement of flow cross section and the increment of flow length by the twisted-tape as follows:

$$u_{sw} = u_0 \frac{\pi d^2}{\pi d^2 - 4w\delta_T} \times \frac{(4y^2 + 2\pi^2)^{0.5}}{2y}$$

$u=u_{sw}$

$\delta=\delta_{sw}$ and $\delta_{cr}=\delta_{cr,sw}$

$q_{cr}=q_{cr,sw}$

2. Fixed Mass Velocity G

$PP_{pump}<PP_{pump,sw}$, $P_{pumpd}<P_{pumpd,sw}$

$G=G_{sw}$

$u=u_{ax,sw}$

$u<u_{sw}$

$\delta>\delta_{sw}$ and $\delta_{cr}>\delta_{cr,sw}$

$q_{cr}<q_{cr,sw}$

This is Common Knowledge.

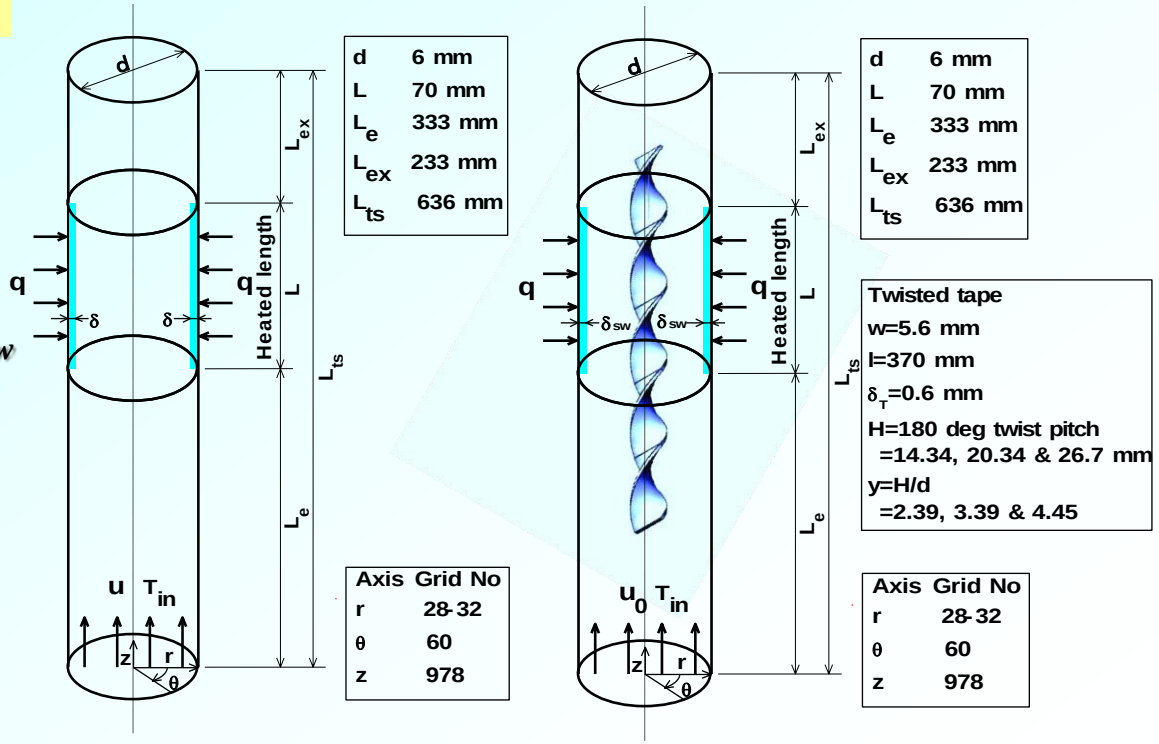

q_{cr} **for CT is the same as $q_{cr,sw}$ for CT with TTI.**

Circular Tube with Twisted-Tape Insert has No Enhancement of CHF.